HHS Public Access

Author manuscript

Isr J Ecol Evol. Author manuscript; available in PMC 2016 September 16.

Published in final edited form as:

Isr J Ecol Evol. 2015 ; 61(1): 37–49. doi:10.1080/15659801.2015.1035508.

Resources, mortality, and disease ecology: Importance of positive feedbacks between host growth rate and pathogen dynamics

Val H. Smith[a], **Robert D. Holt**[b], **Marilyn S. Smith**[c,d], **Yafen Niu**[c,e], and **Michael Barfield**[f]

[a]Department of Ecology and Evolutionary Biology, University of Kansas, Lawrence, KS 66045.

[b]Department of Biology, University of Florida, PO Box 118525, Gainesville, FL 32611-8525. rdholt@ufl.edu. Phone 1.352.392.6917.

[c]Department of Microbiology, University of Kansas Medical Center, Kansas City, KS 66160.

[f]Department of Biology, University of Florida, PO Box 118525, Gainesville, FL 32611-8525. mjb01@ufl.edu. Phone 1.352.392.6914.

Abstract

Resource theory and metabolic scaling theory suggest that the dynamics of a pathogen within a host should strongly depend upon the rate of host cell metabolism. Once an infection occurs, key ecological interactions occur on or within the host organism that determine whether the pathogen dies out, persists as a chronic infection, or grows to densities that lead to host death. We hypothesize that, in general, conditions favoring rapid host growth rates should amplify the replication and proliferation of both fungal and viral pathogens. If a host population experiences an increase in mortality, to persist it must have a higher growth rate, per host, often reflecting greater resource availability per capita. We hypothesize that this could indirectly foster the pathogen, which also benefits from increased within-host resource turnover. We first bring together in a short review a number of key prior studies which illustrate resource effects on viral and fungal pathogen dynamics. We then report new results from a semi-continuous cell culture experiment with SHIV, demonstrating that higher mortality rates indeed can promote viral proliferation. We develop a simple model that illustrates dynamical consequences of these resource effects, including interesting effects such as alternative stable states and oscillatory dynamics. Our paper contributes to a growing body of literature at the interface of ecology and infectious disease epidemiology, emphasizing that host abundances alone do not drive community dynamics: the physiological state and resource content of infected hosts also strongly influence host-pathogen interactions.

Corresponding author. vsmith@ku.edu. Phone 1.785.864.4565.

[d]Current address: Viracor-IBT Laboratories, Lee's Summit, MO 64086. marilyn.smith@viracor-ibt.com. Phone 1.816.251.6668.

[e]Current address: Microarray Core Facility, University of Kansas Medical Center, Kansas City, KS 66160. yniu@kumc.edu. Phone 1.913.588.5575.

The authors declare no conflict of interest or financial interest arising from direct application of this research.

Keywords

disease; fungal pathogens; growth rate; SI models; viral pathogens; HIV

Introduction

Microparasites in their population dynamics within individual hosts are subject to the same ecological processes that shape the abundance and dynamical behavior of all organisms (Andrews 1991; Bohannan 2000; Graham 2008). In this paper, we propose that environmental conditions favoring high internal resource states and rapid host growth rates can be accompanied by the amplification of pathogen replication and proliferation. In some cases, we will argue, these resource-dependent effects can set up a vicious positive feedback loop that elevates morbidity and mortality risks to infected host organisms, with important knock-on consequences for infectious disease dynamics. Moreover, mortality factors imposed on host populations can indirectly alter per capita host resource supplies, and this can modulate within-host pathogen dynamics and alter the expected relationships between mortality regimes and pathogen dynamics (Packer et al. 2003).

The interplay between infectious disease agents and their hosts can be viewed in part as an ecological struggle for potentially growth-limiting resources (Smith 1993a, 1993b; Wodarz 2006; Cressler et al. 2014). All pathogens require the provision of essential nutrients (energy, macronutrients, and micronutrients) to fuel their replication within their host organism, which serves both as a habitat and as a growth medium once infection occurs (Garber 1960; Smith et al. 2005; Smith 2007). Although successful pathogenesis relies upon the ability of invading microbes to acquire the nutrients that are necessary for their reproduction and survival, we currently have only a limited understanding of the *in vivo* resource-dependent physiology and metabolism of most microbial pathogens (Brown et al. 2008). The same is true for other groups of parasites as well.

Resource-ratio theory (Smith 1993a, 1993b) suggests that the supply of key nutrients should strongly influence the outcome of disease, and a study by Cable et al. (2007) suggests that pathogenesis by a diverse set of disease agents (one bacterial, one prion, and three viral pathogens) is strongly moderated by the scaling of metabolism in the host. The direction and pace of host-pathogen interactions should strongly depend upon the rate of host metabolism: the ability of a pathogen to replicate within individual hosts should be strongly constrained by the host organism's resource state, as reflected in the size and turnover rates of the host's internal pools of energy and other resources. These internal host resource dynamics in turn reflect the broad ecological milieu in which the host resides, including its mortality regimes and density-dependent processes. In this paper, we first review experimental evidence for strong effects of host resource state on viral and fungal pathogen replication, and report recent experiments demonstrating this effect. We then explore the implications of these resource effects for host-pathogen dynamics using simple models of infectious disease dynamics (tracking the densities of susceptible and infected hosts and infectious particles). We will in particular focus on how these resource effects indirectly modulate impacts of mortality regimes on pathogen dynamics.

Viral pathogens

Viruses of course are internal parasites of host cells, either free-living (e.g., bacteria), or within multicellular organisms. Viruses reproduce in essentially two ways: either they lyse their host cell, producing a viral burst of size *B*, or (more rarely) free virions are shed from infected but still living and reproductively competent host cells. Host cell resources thus might influence either viral burst size, or viral shedding rates.

Profound effects of host cell condition on viral replication in fact have been reported since the earliest beginnings of experimental virology. For example, Cohen (1949) reviewed early evidence that lag-phase bacterial cells generally produced fewer phage virus particles than exponential-phase populations, and this general sensitivity of viral production to host growth rate has been broadly confirmed for an exceptionally broad range of host organisms and their viral pathogens.

Although the mechanisms underlying the growth-rate modulation of virus replication are not yet fully understood, we hypothesize that growth-rate effects are driven at least in part by differences in the internal resource state of the host. Both host cell metabolic activity and growth rate can regulate the assembly of viral nucleic acids and proteins (Gons et al. 2006; Birch et al. 2012), and strong effects of host population growth stage on viral production have been consistently observed across a diverse range of virus and host types (a selection of examples is summarized in Table 1).

Empirical evidence for effects of host resource state on viral replication

Multiple studies published in the refereed literature provide support for the proposed sensitivity of viral replication to host resource state. For example, Smith et al. (2005) reported strong effects of variation in glutamine supply for host cells on the replication of HIV-1 in laboratory-cultured CEM cells; they found that viral replication was increased by more than 21-fold by increasing the concentration of growth-limiting glutamine from 31 μM to 4 mM in the growth medium. Similarly, strong effects of nutrient availability on viral dynamics have been observed in terrestrial plants (Borer et al. 2010; Lacroix et al. 2014), freshwater phytoplankton (Clasen & Elser 2007), and marine phytoplankton (Wilson et al. 1996; Monier et al. 2012). Strong growth rate control of viral replication also is clearly evident in the negative population density dependence of baculovirus production by insect (*Spodoptera frugiperda*) cells cultivated in laboratory cultures (data from Radford et al. 1997). In Figure 1, we depict virus production by insect cell populations derived from a batch culture grown in a fixed pool of resources; thus, as cell population growth proceeded, there were fewer resources available per capita. Aliquots of the suspended insect cells were harvested at multiple time points during both the logistic and the stationary phases of the batch culture population (see inset), and the susceptible cells harvested at each time point were then exposed to infection with recombinant baculovirus β-galAcNPV. Maximum virus production per cell was then calculated by dividing each maximum volumetric virus yield by the maximum post-infection cell density. The baculovirus virus titer per infected insect host cell declined sharply with increasing host cell population density at the time of infection (TOI) (Figure 1), and thus with increasingly lower cellular resource state at the time of infection.

Another way to indirectly manipulate the resource state of the host is by imposing an additional fixed rate of effective mortality on the host population. In this general scenario, which is derived from resource competition theory (Tilman 1982; Grover 1997), the per capita population growth rate (r, day^{-1}) of the host increases with the internal concentration (Q, pmol cell^{-1}) of the growth-limiting nutrient; r is the difference in the population's intrinsic per capita birth and death rates, but does not include imposed additional mortality. This internal stores model is commonly referred to as the Droop relationship (Droop 1974; Figure 2(a)). The population growth rate should be inversely (but not necessarily linearly) correlated with host population density (N, cells mL^{-1}) (depicted in Figure 2(b); for simplicity, we are ignoring complications such as Allee effects). If an additional population mortality rate is imposed on the host population, the population size will equilibrate (if it can) at the fixed density at which its intrinsic population growth rate matches the imposed additional mortality rate. Thus, at a higher death rate, the population will persist only if it has a correspondingly higher growth rate, requiring a higher availability of resources (lower population density). Higher growth rates will tend to correspond to higher internal resource stores Q and metabolic rates in the host cells, and parasites can be expected to exploit this elevated resource availability.

In earlier papers (Packer et al. 2003; Holt 2008) we have shown in SI (Susceptible-Infected) models that imposing density-independent mortality on a host-pathogen system can depress the basic reproductive number R_0 of the pathogen (the number of secondary infections generated by one infected host when infection is rare), and also the equilibrial prevalence of the infection. This could imply for instance that predation can prevent epidemics and lower the prevalence of persisting pathogen populations. Comparable effects can arise when predators attack hosts that support vectors that transmit infectious disease agents (Levi et al. 2012). However, these analyses have ignored resource dependencies in transmission dynamics mediated by changes in host internal resource states. In the model presented below we will examine how such dependencies alter the relationship between density-independent mortality and infection dynamics.

Experimentally, one way to indirectly impose mortality upon a population of host cells is via physical dilution, either in continuous (i.e., chemostat) or in semi-continuous cultures of suspended cells. A chemostat consists of a container with a constant volume of a well-mixed liquid medium containing a population of cultivated cells, a portion of which flows out when new sterile medium is added at the same fixed rate (the dilution rate D, expressed as the proportion of inflowing fresh medium relative to the total culture volume per unit time). Organisms lost through the outflow are removed from the system, and therefore the dilution rate (D, in units of hr^{-1} or day^{-1}) is effectively a per capita mortality rate imposed upon the chemostat population. The population growth rate r must match D in order for the population to persist. At high dilution rates, host density drops, resulting in more resources per host and allowing them to replicate more rapidly (Figure 2(b)). Thus, this mortality-induced change in resource state should indirectly boost pathogen replication rates.

For example, Middelboe (2000) established steady-state cultures of the bacterium *Pseudoalteromonas sp.* in which the per capita bacterial host cell population growth rate (r, hr^{-1}) just equaled the dilution rate D of the chemostat, for a series of three different dilution

rates. They then took aliquots from each of these different steady-state cultures, briefly exposed each aliquot to infection by bacteriophage, pelleted and washed the cells of unadsorbed virus using artificial seawater, resuspended the washed cells, and then measured virus production. A strongly positive relationship was indeed observed between the pre-infection population growth rate of the bacterial host, and the subsequent post-infection burst size, B, of this viral pathogen (Figure 2(c)).

Experimental tests for effects of host resource state on retrovirus replication —In order to explore the generality of the growth-rate stimulation of virus production that was observed by Middelboe (2000) and in the studies compiled in Table 1, we experimentally infected a human T-cell line (CEM cells) grown in semi-continuous culture at four different dilution rates. These CEM cells were grown in semi-continuous cultures, in which a fraction f of the total culture volume was removed manually once per day, and was immediately replaced with fresh sterile medium. The steady-state host cell populations were then infected with the retrovirus SHIV89.6P, a pathogenic chimera between HIV-1 and a simian immunodeficiency virus (SIV). As in the case of the chemostat cultures described in the previous section, in persisting host populations, the per capita population growth rate of the host cells contained within the semi-continuously diluted culture vessels should just match the dilution-imposed mortality rate at equilibrium. A description of our experimental methods follows.

Cells, virus, and growth medium: CEM cells were obtained from the NIH AIDS Research and Reference Reagent Program. The CEM cells were cultivated in AIM-V ® serum-free medium (Invitrogen ®, Carlsbad, CA). O. Narayan, University of Kansas Medical Center, kindly supplied the SHIV89.6P strain.

Dilution rate manipulations: Uninfected susceptible CEM cells were cultivated to a large volume at a temperature of 37°C in batch cultures containing the growth medium above, and counted. These cells were then used to inoculate eight flasks containing 20 mL of medium with a constant starting density of 5×10^5 cells mL^{-1}. Duplicate flasks were then allocated to four dilution rates (f = 0.125, 0.200, 0.275, and 0.350 day^{-1}) with daily medium changes. These semi-continuous dilution rates (f) were calculated as the volume of culture medium that was removed and replaced once daily, divided by the total culture volume (Holm & Armstrong 1981). Cells in each flask were counted at intervals of 2-3 days (just prior to semi-continuous dilution on each sampling date). On day 11, one half of the steady-state cells from each flask was pelleted and resuspended in 1 mL of AIM-V ® medium containing SHIV89.6P (virus titer $10^{4.8}$ mL^{-1}) for 2 hr at 37°C, resulting in a variable multiplicity of infection (MOI) ranging from 0.015 (at the dilution rate 0.125 day^{-1}) to 0.05 (at the dilution rate 0.35 day^{-1}). The infected cells were then pelleted, washed once in pre-warmed Hank's Balanced Salt Solution (Invitrogen ®), and resuspended in a constant volume (10 mL) of AIM-V ® medium, restoring them to the day 11 cell concentration that had been obtained for each growth rate treatment. The infected cells were then incubated at 37°C for 48 hr, at which time the cells were pelleted. Aliquots of cell-free virus supernatant were frozen at −80°C for viral RNA purification (QIAamp ® viral RNA mini kit, QIAgen ®), and two aliquots of the total cells were processed for isolation of DNA by QIAgen DNA columns

and for total RNA by Trizol ® (Invitrogen). Purified RNAs were stored at −80°C and purified DNA was stored at −20°C.

Real-time PCR: Virus particles in the supernatant were quantified using real-time RT-PCR from a defined proportion of the total RNA purified from a known volume of the total supernatant volume. Proviral DNA was quantified by real-time PCR from the DNA extracted from the cells of each flask, and was normalized to the amount of cellular DNA in the reaction (Mackay et al. 2002; Smith et al. 2002).

Experimental results: As predicted, SHIV replication in our CEM cells was exceptionally sensitive to host cell population growth rate. The production of SHIV increased from a mean of 0.03 viral RNA copy per cell at the lowest dilution rate, to a mean of 11 viral RNA copies per cell at the highest dilution rate (Figure 2(d)), a 300-fold increase with less than a 3-fold increase in dilution rate.

The evidence in Table 1 and Figures 1-2 together confirms that there is a very strong potential for the host cells' physiological state to influence viral pathogen dynamics, and for increases in imposed mortality to indirectly boost the viral production rate per infected host cell. The next section provides evidence for comparable influences of resource limitation on fungal pathogen dynamics.

Fungal pathogens

Growth state (and its corresponding physiological state) can also strongly influence interactions between fungal pathogens and their host organisms. In individual vascular plants, Relative Growth Rate is analogous to the per capita growth rate of a population (r, day^{-1}), and RGR correlates positively with tissue concentrations of growth-limiting nutrients, especially phosphorus and nitrogen (Ågren 2008). Increased resource availability within the cells of a plant host should facilitate fungal proliferation. Nitrogen availability has been demonstrated to control multiple aspects of fungal infections in numerous vascular plant species, including fungal colony formation and spore production (see Table 2 in Hoffland et al. 2000). Solomon et al. (2003) and Smith (2007) provide additional information on the general effects of nutrient supplies on the dynamics and outcome of fungal diseases in terrestrial plants.

Compelling evidence for a very strong coupling between host resource state and fungal pathogen dynamics can be found in the algal disease literature. For example, chytrid fungi are highly virulent parasites on diatoms: these fungi can infect more than 90% of the susceptible cells in a population, with each chytrid infection quickly killing its host (Gsell et al. 2013). Bruning (1991a) used semi-continuous culture methods to study interactions between the diatom *Asterionella formosa* and a virulent chytrid pathogen, *Rhizophydium planktonicum*. An exceptionally strong positive correlation was observed between the per capita population growth rate (r, day^{-1}) of light-limited *A. formosa* cells and the reproduction of their associated chytrid parasites, as measured by the number of fungal zoospores per mature sporangium (Figure 3). An increase in light availability thus greatly increased the production rate of fungal zoospores by infected diatoms.

In a related set of experiments (data not shown), Bruning (1991b) found that phosphorus-limited cells of the diatom *A. formosa* were less susceptible to infection with zoospores of their *R. planktonicum* fungal parasite than were non-phosphorus-limited host cells. The sporangia on phosphorus-limited diatoms produced substantially fewer zoospores, but the development time of the sporangia was only slightly reduced. As a result of these resource supply effects, *R. planktonicum* reached lower growth rates at a given host density, and survival of the parasite required higher host densities, when its host *A. formosa* was phosphorus-limited (van Donk & Bruning 1995).

Thus, as with the viral pathogens discussed in the previous section, the dynamics of fungal pathogens appear to be very tightly linked to resource availability and the physiological state of their host.

Development of a simple disease modeling framework incorporating resource availability

The data in Figures 1-3 suggest that host-state-driven modulation of pathogen growth and reproduction can be a dramatic feature of host-pathogen interactions. This matches a growing recognition that resource dependencies can be significant “bottom-up” drivers of infectious disease dynamics (e.g. Hall et al. 2009; Cressler et al. 2014; Hurtado et al. 2014). In the next section, we develop a simple model that encapsulates the effects shown in the empirical examples reviewed above, and we use this model to explore further the indirect effects of mortality regimes on infectious disease dynamics. Despite its simplicity, the model demonstrates that bottom-up resource effects can lead to alternative stable states and to unstable dynamics, and therefore can influence how host mortality indirectly affects disease dynamics.

Disease model

A simple dynamic model structure that is commonly explored in the mathematical virology literature (e.g., Perelson et al. 1996; Neumann et al. 1998; Perelson & Nelson 1999; Davenport et al. 2006) is the following:

$$\frac{dS}{dt} = F(S) - mS - \beta SV \quad (1)$$

$$\frac{dI}{dt} = \beta SV - (m+\alpha) I \quad (2)$$

$$\frac{dV}{dt} = pI - uV \quad (3)$$

where S, I, and V are the concentrations of susceptible healthy hosts, infected hosts, and free virions (or, in general, pathogen particles, as long as their production is proportional to the density of infected hosts), respectively. This model is simpler in some respects than other recent theoretical explorations of resource effects in infectious disease dynamics (e.g., Hurtado et al. 2014; Cressler et al. 2014), but it leads to complementary results.

The death rate of uninfected host cells is m, and α is the additional cell mortality due to infection. As this model is generally used, m is the natural susceptible cell death rate, but instead it can also include an imposed increased cell death rate, such as the dilution rate in a chemostat. The quantity p is the rate of production of free infectious particles per infected host cell, and u is their loss rate; infected hosts do not recover, nor do they give birth to susceptible hosts. For viruses that shed, p measures the rate of shedding, and is not directly dependent on host mortality. For viruses that replicate by bursting, p will depend on both host mortality and burst size. For our purposes, we can keep this dependence implicit, rather than explicit. [One possible form would be $p = B(q'\alpha + qm)$, where q' and q are the fractions of host cell mortality events which generate viruses; the first term is likely to dominate p.] The quantity β scales the rate at which healthy host cells pick up free pathogens and become infected (we ignore here the often trivial loss due to this uptake from the pool of free pathogens). The recruitment term, $F(S)$, represents the rate at which new susceptible cells are added, and may for example be simply a constant λ, the supply rate of new susceptible hosts per unit time. Alternatively, for populations of hosts that are self-recruiting, $F(S)$ may be an expression such as $S(b - cS)$ (logistic growth), where b is the per capita cell birth rate at low density, and c reflects density dependence in growth (for instance due to a limited pool of resources being available). (If density dependence is in births, then we assume that either $b - cS \geq 0$, which is always true as long as it is true for the initial value of S.) We assume for simplicity for the most part that infected hosts do not directly contribute to density dependence in the susceptible hosts. Moreover, we assume that infected hosts have a relatively short lifespan, so that their internal resource states change little from the time of infection until death.

This model is frequently used for virus infections within a host organism, in which case S and I are respectively susceptible and infected host cells, and V is the abundance of free virions. This simple model could also describe the infections in cell cultures of Figure 2(d), but the model can broadly pertain to many host-pathogen systems where there is no acquired immunity, and infection occurs via an environmental pool of infective propagules. For instance, this model (or modifications of it) can describe a chytrid fungus infecting diatoms as in Figure 3. In this special case, S and I are susceptible and infected diatoms, respectively, and V is the concentration of free fungal zoospores. A zoospore can attach to and infect a healthy diatom, which can lead to the development of a sporangium that produces zoospores asexually and releases them (sexual reproduction can also occur in chytrid fungi, but often asexual reproduction dominates; van Donk & Ringleberg 1983). The above model would apply to this system as long as the production of zoospores is proportional to the number of infected diatoms, and uptake of zoospores by diatoms is quantitatively negligible, relative to other processes. Gerla et al. (2013) uses a model similar to this one, but including a variable for the density of sporangia (plus an explicit equation for a resource, which we include implicitly in our model through its effect on p). Equations (1)-(3) could also apply both to

fungi that reproduce intracellularly and to some fungi that attack multicellular organisms (e.g., cladocerans), in which case S and I are susceptible and infected host organisms. Of course, many fungi (and other pathogens) have more complicated life histories, and would require a more complex model.

If a self-recruited population of host cells is to persist, then we must have $b - cS \geq m$, so the net growth of susceptible host cells must at least match losses. Any differences in growth rate are likely to be reflected as differences in the internal states of the proliferating hosts, resulting in altered intracellular environments experienced by pathogens invading them. Resource-rich infected host cells would be expected to produce more infectious particles per cell than would more resource-poor cells (Clasen & Elser 2007), either by continual shedding or by bursting (Holt & Barfield 2006). This implies that there should be a relationship between host growth conditions (expressed quantitatively by the magnitude of $b - cS$) and the production rate p of infectious particles per infected host cell, which could also lead to an emergent indirect relationship between mortality imposed on the host and this production rate.

Although there are exceptions, the value of pathogen production rate p (or burst size B) has frequently been treated as a constant in diverse virus modeling efforts performed during the past two decades (Bonhoeffer et al. 1997; Nowak & May 2000; Lloyd 2001; Wu et al. 2001; Davenport et al. 2002; Gilchrist et al. 2004; Våge et al. 2013). In contrast, pathogen production rate has been recognized to be a variable in the modeling of fungal pathogens for more than two decades (e.g., chytrid fungi: Bruning 1991a, 1991b). Based upon the data in Figures 1-3, we hypothesize that burst size B is not constant but variable, and in particular is sensitively dependent upon the physiological and nutritional state of the infected host cell for both fungal and viral pathogens.

If we assume that the free pathogen particles equilibrate much faster than the host cells, the pathogen number will approximately track the value obtained by setting $dV/dt = 0$, which is $V^* = pI/u$ (we will use asterisks to indicate equilibrium values). This can be substituted into the dS/dt and dI/dt equations. For the logistic form of $F(S)$, this gives the system

$$\frac{dS}{dt} = (b - cS)\, S - mS - \beta' SI \quad (4)$$

$$\frac{dI}{dt} = \beta' SI - (m+\alpha)\, I, \quad (5)$$

where $\beta' = \beta p/u$. For these equations, the net growth rate of susceptible cells is $g = b - cS$. If pathogen production rate p is an increasing function of this growth rate, then so is the effective rate of transmission β', so we will denote this functional relationship as $\beta'(g)$. If infected cells (and therefore also free pathogens) are rare, then susceptible cells will reach the disease-free equilibrium $S_0^* = (b - m)/c$. At this equilibrium, from Equation (5), the

condition for the infected cells to increase is that $\beta'(g_0^*)\,S_0^* > m+\alpha$, where $g_0^* = b - cS_0^*$, which is equal to m.

By varying m (for example, by removing cells at a constant rate via dilution, which effectively increases m), the net growth rate at equilibrium is also varied, and presumably the metabolic state of the cells. As noted earlier, one general question we are interested in examining is revisiting the impact of density-independent mortality (e.g., due to a generalist predator) on pathogen dynamics, to discern whether or not bottom-up effects of resources on pathogen production can reverse the expected negative effect of increased mortality on disease prevalence and persistence.

For this system, we can also find the basic reproduction number R_0, which is the average number of susceptible cells infected by free pathogens produced by a single infected cell, assuming infection is rare. When infection is rare, an infected cell infects susceptible cells at a rate of $\beta' S_0^*$ and has an average lifetime of $1 / (m + \alpha)$, giving

$$R_0 = \frac{\beta'(g_0^*)\,S_0^*}{m+\alpha} = \frac{\beta'(m)\,(b-m)}{c\,(m+\alpha)}. \quad (6)$$

For the infection to increase when rare, R_0 must be greater than 1, which gives the same condition as derived above. R_0 decreases with increasing m in three circumstance: i. β' does not depend on m; ii. β' decreases with increasing m, or iii. β' increases with m, but not at a sufficient rate. By contrast, if β' increases strongly with increasing m, as in the empirical examples shown in Figures 2 and 3, then it is possible for R_0 to increase with increasing m for some ranges of m (R_0 drops to 0 at $m = b$, so it drops with increasing m for sufficiently high m). The condition for R_0 to increase with increasing m is

$$\frac{d\,ln\,\beta'(m)}{dm} > \frac{b+\alpha}{(b-m)\,(m+\alpha)}. \quad (7)$$

To go beyond these results requires specifying the functional form of β'. We consider two possibilities. For the first, β' is an exponential function of g (as suggested by the data in Figures 2(b) and 2(c)), so $\beta'(g) = \beta_0' \exp\{kg\}$. At the disease-free equilibrium, $g = m$, so $\beta'(m) = \beta_0' \exp\{km\}$, and the left side of (7) is constant (k). If $b < a$, the right side increases with increasing m, so for R_0 to increase with m requires that it does so for $m = 0$, which requires $k > (b + a) / (ba)$ [the right side of (7) for $m = 0$]. If this is true and $R_0 < 1$ for $m = 0$ but R_0 peaks at a value above 1, then it is possible for increasing m to allow a pathogen to become established that could not do so otherwise (there are two values of m for which $R_0 = 1$, with $R_0 > 1$ between them; Figure 4(a)). If $b > a$, the right side of (7) decreases with increasing m for small m, reaching a minimum value of $4 / (b + a)$ at $m = (b - a) / 2$ and increasing for higher m. Therefore, in this case it is possible for R_0 to decrease at small m [if $k < (b + a) / (ba)$], then increase at intermediate m [if $k > 4 / (b + a)$] before

decreasing at large m. In this case there can be three values of m for which $R_0 = 1$, with $R_0 > 1$ at low m and for a range of higher m, as in Figure 4(b).

The bottom line of these analyses is that if effective transmission can increase with increasing host growth rates, then starting with low mortality, an increase in mortality imposed on all hosts can facilitate establishment of a pathogen, because this increased mortality boosts host growth rates and thus the transmission efficacy of infected hosts. At sufficiently high mortality, however, the pathogen cannot persist. In some cases, there are more complex patterns of establishment along gradients in mortality, with establishment possible within distinct mortality regimes, one low, and one higher; we show an example in Figure 4(b).

Given that the pathogen persists, the net growth rate of susceptible host cells is no longer equal to m, so we have to return to $\beta' = \beta'(g) = \beta'(b - cS)$. The equilibrium value of susceptible cells, S^*, can be found by setting the derivative in (5) to 0, giving $S^* = (m + \alpha) / \beta'(b - cS^*)$. This can have multiple solutions. For example, if $\beta'(g) = \beta_0^* exp\{kg\}$, then the equilibria satisfy $S^* exp\{-kcS^*\} = exp\{-kb\}(m+\alpha)/\beta_0'$. The left side is 0 for $S^* = 0$ and approaches 0 as S^* approaches infinity, and is positive otherwise. If its peak is greater than the right side, then there are two solutions (otherwise there are none). This can happen because the pathogen reduces S and therefore increases g, which increases β'. If the pathogen starts out rare and can increase, it can reach a low S equilibrium, at which the growth rate is low, so β' is low, which restricts further growth of the pathogen. If the pathogen could reach high levels, then it would reduce S to low levels, at which g and therefore β' are high, facilitating higher levels of the pathogen. The upper equilibrium tends to be unstable, and, depending on initial conditions, this instability can result in loss of the pathogen or movement toward the lower equilibrium. The lower equilibrium can be unstable, which can result in persistent cycles (Figure 5(a), which has the same parameters as Figure 4(a)), or in some cases in loss of the pathogen.

Isoclines

In Figure 5(b), we depict the isoclines for this case. It may be useful to lay out the reason for the isoclines to have the shapes shown there. The isocline for the infection (I) is actually a pair of vertical (dashed) lines, with a positive growth rate for I between these two lines. At low S, the infection declines because there are two few healthy cells available to sustain the infection. At high S, the infection declines because healthy hosts are competing among themselves, reducing their growth rate and hence the ability of the pathogen to replicate itself. The isocline for the healthy portion of the population (S) has a hump. This resembles the familiar humped isocline of the classical Rosenzweig-MacArthur predator-prey model, but the positive rise of the isocline to the left occurs for a quite different reason than in that model (viz., a saturating functional response). As host numbers rise, they compete among themselves. This in turn reduces the rate at which infected hosts can produce infective propagules, which means more infected hosts are required for the susceptible portion of the population to be in equilibrium.

Holt & Barfield (2013) recently examined a system which superficially seems very different than this host-pathogen system, namely models for food chains in which the abundance of the basal resource (a plant) entered directly into the functional response coupling the predator and herbivore populations. This led to isoclines that qualitatively resemble those of the above model (e.g., Figure 9 in Holt & Barfield 2013 is quite comparable in form to Figure 5(b) in the current paper), permitting alternative states and unstable limit cycle dynamics.

The second functional form of β' that we examined is a linear increase, so that $\beta'(g) = \beta_0' + kg$, which is analytically more tractable. In this case, the condition for R_0 to increase with increasing m is $k/\left(\beta_0' + km\right) > (b+\alpha)/[(b-m)(m+\alpha)]$. The condition at m = 0 is that $k/\beta_0' > (b+\alpha)/(b\alpha)$. If this is true, then R_0 increases with m until $m = \sqrt{(b+\alpha)(\alpha - \beta_0'/k)} - \alpha$, above which it decreases. Therefore, it is possible for increasing m to facilitate pathogen establishment (for m below this peak), and for there to be two values of m for which R_0 = 1 (if the value at 0 is less than 1 but the peak is greater than 1), as we show in Figure 6(a). (It is not possible for there to be more than two, however.)

As with the exponential form of β', it is possible to get two equilibria, such as in the isocline diagram in Figure 6(c), which has parameters corresponding to Figure 6(a) (and m = 0.2). In this case, the right equilibrium (indicated by the filled circle) is stable. The left equilibrium is unstable, and starting near it, the system sometimes moves to the stable equilibrium, as shown in Figure 6(b) (in the figure we show only the initial part of the trajectory; the oscillations continue to decrease until the stable equilibrium is reached). In other cases, starting near the unstable equilibrium results in loss of the pathogen. This can happen because R_0 < 1, as shown in Figure 6(a) (the × corresponds to m = 0.2, the value for Figures 6(b) and 6(c)). In Supplemental Material Appendix A, we also show that it is necessary that R_0 < 1 for there to be two feasible equilibria (two equilibria with S^* and I^* > 0) for linear β'.

Changes in equilibrial prevalence with increasing m

In Susceptible-Infected models with fixed transmission rates, increases in mortality (due say to generalist predators) on hosts reduces the equilibrial prevalence of infectious diseases (Packer et al. 2003; Holt 2008). Adding acquired immunity, with density dependence, can permit low levels of predation to actually increase disease prevalence (Holt & Roy 2007). How does host-growth dependence in disease transmission alter the relationship between mortality and disease prevalence? In Appendix A (Supplemental Material), we derive the equilibria of a system like Equations (4) and (5), but more general, in that the mortality of susceptible cells is m_S and that of infected cells is m_I, rather than both being set equal to the same rate m. The equilibria are that S^* is the solution of $S^* = (m_I + \alpha)/\beta'(S^*)$ and $I^* = (b - m_S - cS^*)/\beta'(S^*)$, which gives an equilibrium prevalence (proportion of cells infected) of

$$p^* = \frac{I^*}{S^* + I^*} = \frac{b - m_S - cS^*}{(m_I + \alpha) + (b - m_S - cS^*)} = \frac{b - m_S - cS^*}{b + \alpha + m_I - m_S - cS^*}.$$

In Appendix A (Supplemental Material), we also show that an equilibria of this system is unstable (in a way that causes the system to move monotonically away from the equilibria, resulting in movement to the neighborhood of a different equilibrium) if $d(\beta' S^*) / dS^* < 0$. We show there that the equilibrium prevalence always decreases with increasing m_S when m_I is constant, with increasing m_I when m_S is constant, or with increasing m when $m_S = m_I = m$, for any stable equilibrium or for that matter equilibrium around which the system oscillates (equilibria not satisfying the above inequality).

The bottom line of this analysis is that increases in mortality in this system always depress the equilibrial prevalence of the infection, despite the complexities noted above in effects of mortality on R_0. Hence, the results of Packer et al. (2003) with respect to effects of generalist predators on equilibrial disease prevalence still hold when transmission increases with increasing host growth rates.

However, we caution that this result might depend on particular assumptions made in the above model. For instance, we assumed that density dependence in the host (emerging say from resource competition) was driven by the abundance of susceptibles, not by infectives. In effect, this assumes that infected individuals stop consuming resources (so the pathogen in its own dynamics experiences the within-host resource environment of the host that is present at the moment of infection). An alternative assumption would be to allow density dependence to occur from infected individuals that continue post-infection to interact demographically and ecologically with susceptibles (so the density dependence depends on $N = S + I$ rather than S; this is comparable for instance to an assumption made in the model explored by Hurtado et al. 2014). For instance, Equations (4) and (5) might become

$$\frac{dS}{dt} = (b - c(S+I))\,S - mS - \beta' SI \quad (8)$$

$$\frac{dI}{dt} = \beta' SI - (m+\alpha)\,I \quad (9)$$

where now $\beta' \equiv \beta'(g) = \beta'(b - c(S + I))$. Since R_0 is calculated when infection is rare, the previous results for the form of R_0 for the model of Equations (4) and (5) also apply to Equations (8) and (9). In particular, our conclusions about nonlinearities in R_0 as a function of morality imposed on the host (e.g., Figure 4) still hold. However, the equilibria and isoclines for this system will be more complicated, and little can be done analytically. For the linear form of β', we obtained closed-form expressions for the isoclines. In this case, the isocline of Equation (8) (plotted as I as a function of S, as in Figure 6(c)) is shifted to the left (lower S) by making the density dependence depend on N instead of S. The isoclines of Equation (9) are no longer vertical lines; the S-axis intercepts are identical to those with S density dependence, but as I increases the lower S value increases and the upper S value decreases, until they join to produce a continuous curve (for the parameters of Figure 6(c), they meet at about $I = 25$, well above the I values in the figure; for the values in the figure, the dashed lines would only be modestly tilted inward with increasing I). The use of this

form of density dependence does not change the behavior of the system of Figure 6(c); the equilibria are merely shifted. For stronger density dependence (higher c), making the density dependence depend on N can result in loss of either or both equilibria.

Discussion and Conclusions

Population ecology has long focused on the dynamics of abundance, but there has been an increasing recognition of the need to monitor changes in internal resource (and other) states of the organisms involved, ranging from the Droop internal stores model of resource-limited phytoplankton growth (Droop 1974; Grover 1997), to maternal effects in models of population cycles (Inchausti & Ginzburg 2008), to the density dependence of cellular metabolism (DeLong & Hanson 2009), to the implications of individual energy and material budgets (Brown et al. 2004; Kooijman 2010). In the present study, we have tried to place disease ecology into this broader context, recognizing that the metabolic state of interacting organisms also has a major role to play in the dynamics of species interactions. Researchers are increasingly recognizing that resource dependencies can strongly modulate the dynamics of interactions between hosts and parasites. The examples we review above demonstrate that host resource state can have very strong impacts on pathogen abundance. Our own experimental study demonstrates that an increase in mortality (in our case resulting from imposed dilution in a cell culture) can indirectly very strongly boost the production of viral pathogens (see Figure 2(d)). Both in this example, and in zoospore production in infected diatoms (Figure 3), pathogen production does not just increase with increasing mortality, but increases at an accelerating rate. This suggests that rather small changes in mortality regimes can have large and surprising impacts on pathogen dynamics. An interesting question for future investigation would be to tease out the physiological mechanisms underlying these strongly nonlinear responses.

Authors of several recent papers have used theoretical models to explore resource effects on host-pathogen dynamics. Despite differences in model assumptions, all lead to a consistent set of conclusions. Hurtado et al. (2014), for instance, track a logistic resource explicitly, and assume that infected and susceptible hosts all consume that resource at the same rate. Cressler et al. (2014) characterize the interaction between an immune response and pathogens within a host as a predator-prey interaction, where both the “predator” and its “prey” can depend on host resources. Gerla et al. (2013) developed a Susceptible-Infected model for a diatom host-chytrid parasite system that explicitly includes reproduction of the parasite on hosts and free-living infective parasite stages. A distinguishing feature of their model is that the rate of parasite production by infected hosts increases with increasing nutrient availability to those hosts, and that the nutrient is replenished in a semi-chemostat fashion. All of these models demonstrate properties parallel to those we have shown in our simple model, such as the emergence of alternative equilibria and unstable dynamics. An increase in host death rates does not automatically imply that pathogen persistence is impaired (as in Packer et al. 2003), but instead can provide an indirect boost to pathogen R_0 and thus its persistence, because with fewer hosts present, each remaining host when infected can generate more pathogens before it itself dies.

Our review of the empirical literature and our own experimental results, together with these theoretical studies, show that the direction and pace of host-pathogen interactions is strongly dependent upon the rate of host cell metabolism, and that the physiological state of infected plant and animal hosts can profoundly influence the dynamics and outcome of infectious disease. Resource quantity and quality not only can modulate the virulent effects of pathogens on the survivorship of infected hosts, but also can directly influence pathogen production (Hall et al. 2009), which then can modulate the emergent effects of mortality regimes in host-pathogen dynamics. We suggest that it will be valuable to assess more broadly, across a wide range of host-pathogen systems, the dependence of pathogen load and burst size on nutrient availability to hosts. Future studies quantifying pathogen titer levels in response to altered host resource state are highly desirable and very strongly warranted because important aspects of disease dynamics may be unrecognized or overlooked if key ecological interactions between hosts, pathogens, and their shared resources are not explicitly taken into account (Gerla et al. 2013). Nutrient availability and host resource content surely play an important role in shaping within-host competition among pathogen strains, as well as across-host transmission success. These effects have largely unexplored implications for the evolution of virulence, as well as of host and parasite life cycles (see Gsell et al. 2013 and LaCroix et al. 2014 for examples), for instance by altering competitive interactions in coinfection (LaCroix et al. 2014).

There are also strong public health and applied implications of this issue. Research that links resource availability to pathogen replication and virulence can provide important new insights into the resource modulation of host-pathogen dynamics, and potentially enhance our ability to predict the persistence, spread, and outcome of infectious disease in applied settings. For example, although the cellular mechanisms responsible for the patterns shown in Figure 2(d) are not yet clear, we speculate that diet- or disease-induced variations in the metabolic state of susceptible target cells may have important implications for *in vivo* HIV dynamics.

In addition, humans are enriching many environments with excess nitrogen and phosphorus, and this bottom-up effect can be predicted to alter disease dynamics. Plant hosts with high tissue concentrations of phosphorus and elevated metabolic rates can harbor greater pathogen loads (Clasen and Elser 2007; Cronin et al. 2010); environmental eutrophication can lead to such nutrient enrichment and indirect facilitation of infection (e.g., by viruses in a successional grassland, Borer et al. 2014). Moreover, anthropogenic landscape change can shift community composition so as to favor “fast-lived” species, as in early succession, and by exhibiting rapid growth, such fast-lived individuals could be more susceptible as pathogen hosts and sustain greater intensities of infection, relative to more slow-lived individuals (Johnson et al. 2010, 2012; Cronin et al. 2014). Across the Tree of Life, fast-living and resource-rich host phenotypes can be expected be more susceptible, more competent, more tolerant, and more likely to support greater vector and pathogen populations (Cronin et al. 2010).

Supplementary Material

Refer to Web version on PubMed Central for supplementary material.

Acknowledgments

This research was supported by NSF grants DMS–0342239 to VHS and MSS and DMS-1220342 to RDH, and NIH grants GM-60792 and GM-083192 to RDH. VHS and MSS thank J. Elser, Y. Kuang, and the Arizona State University disease ecology group. RDH thanks the University of Florida Foundation for additional support, and we thank Vitrell McNair for editorial assistance.

References

Ågren G. Stoichiometry and nutrition of plant growth in natural communities. Annu. Rev. Ecol. Evol. Syst. 2008; 39:153–170.

Andrews, JH. Comparative ecology of microorganisms and macroorganisms. Springer-Verlag; New York (NY): 1991.

Birch EW, Ruggero NA, Covert MW. Determining host metabolic limitations on viral replication via integrated modeling and experimental perturbation. PLoS Comput. Biol. 2012; 8(10):e1002746. doi: 10.1371/journal.pcbi.1002746. [PubMed: 23093930]

Bohannan, BJM. Effect of resource supply rate on host-pathogen dynamics.. In: Bell, CR.; Brylinsky, M.; Johnson-Green, P., editors. Microbial biosystems: New frontiers. Proceedings of the 8th International Symposium on Microbial Ecology. Atlantic Canada Society for Microbial Ecology; Halifax: 2000. p. 595-601.

Bonhoeffer S, May RM, Shaw GM, Nowak MA. Virus dynamics and drug therapy. Proc. Natl. Acad. Sci. U.S.A. 1997; 94:6971–6976. [PubMed: 9192676]

Borer ET, Seabloom EW, Mitchell CE, Power AG. Local context drives infection of grasses by vector-borne generalist viruses. Ecol. Lett. 2010; 13:810–818. [PubMed: 20482583]

Borer ET, Seabloom EW, Mitchell CE, Cronin JP. Multiple nutrients and herbivores interact to govern diversity, productivity, composition, and infection in a successional grassland. Oikos. 2014; 123:214–224.

Bratbak G, Jacobsen A, Heldal M, Nagasaki K, Thingstad F. Virus production in *Phaeocystis pouchetii* and its relation to host cell growth and nutrition. Aquat. Microb. Ecol. 1998; 16:1–9.

Brown JH, Gillooly JF, Allen AP, Savage VM, West GB. Toward a metabolic theory of ecology. Ecology. 2004; 85:1771–1789.

Brown SA, Palmer KL, Whitely M. Revisiting the host as a growth medium. Nature Rev. Microbiol. 2008; 6:657–666. [PubMed: 18679171]

Bruning K. Infection of the diatom *Asterionella* by a chytrid. I. Effects of light on reproduction and infectivity of the parasite. J. Plankton Res. 1991a; 13:103–117.

Bruning K. Effects of phosphorus limitation on the epidemiology of a chytrid phytoplankton parasite. Freshw. Biol. 1991b; 25:409–417.

Cable JM, Enquist BJ, Moses ME. The allometry of host-pathogen interactions. PLoS ONE. 2007; 2(11):e1130. doi:10.1371/journal.pone.0001130. [PubMed: 17987117]

Chillakuru RA, Ryu DDY, Yilma T. Propagation of recombinant vaccinia virus in HeLa Cells: Adsorption kinetics and replication in batch cultures. Biotechnol. Prog. 1991; 7:85–92. [PubMed: 1367173]

Clasen JL, Elser JJ. The effect of host *Chlorella NC64A* carbon:phosphorus ratio on the production of *Paramecium bursaria Chlorella Virus-1*. Freshw. Biol. 2007; 52:112–122.

Cohen SS. Growth requirements of bacterial viruses. Bacteriol. Rev. 1949; 13:1–24. [PubMed: 16350126]

Cressler CE, Nelson WA, Day T, McCauley E. Disentangling the interaction among host resources, the immune system and pathogens. Ecol. Lett. 2014; 17:284–293. [PubMed: 24350974]

Cronin JP, Welsh ME, Dekkers MG, Abercrombie ST, Mitchell CE. Host physiological phenotype explains pathogen reservoir potential. Ecol. Lett. 2010; 13:1221–1232. [PubMed: 20618842]

Cronin JP, Rúa MA, Mitchell CE. Why is living fast dangerous? Disentangling the roles of resistance and tolerance of disease. Am. Nat. 2014; 184:172–187. [PubMed: 25058278]

Davenport MP, Fazou C, McMichael AJ, Callan MF. Clonal selection, clonal senescence, and clonal succession: the evolution of the T cell response to infection with a persistent virus. J. Immunol. 2002; 168:3309–3317. [PubMed: 11907087]

Davenport MP, Zhang L, Shiver JW, Casmiro DR, Ribeiro RM, Perelson AS. Influence of peak viral load on the extent of CD4+ T-cell depletion in simian HIV infection. J. Acquir. Immune Defic. Syndr. 2006; 41:259–265. [PubMed: 16540926]

DeLong JP, Hanson DT. Metabolic rate links density to demography in *Tetrahymena pyriformis*. ISME J. 2009; 3:1396–1401. [PubMed: 19571891]

Droop MR. The nutrient status of algal cells in continuous culture. J. Mar. Biol. Assoc. U.K. 1974; 54:825–855.

Garber ED. The host as a growth medium. Ann. NY Acad. Sci. 1960; 8:1187–1194. [PubMed: 13703461]

Gerla DJ, Gsell AS, Kooi BW, Ibelings BW, van Donk E, Mooi JWM. Alternative states and population crashes in a resource-susceptible-infected model for planktonic parasites and hosts. Freshw. Biol. 2013; 58:538–551.

Gilchrist MA, Coombs D, Perelson AS. Optimizing within-host viral fitness: infected cell lifespan and virion production rate. J. Theor. Biol. 2004; 229:281–288. [PubMed: 15207481]

Gons HJ, Hoogveld HL, Simis SGH, Tijdens M. Dynamic modelling of viral impact on cyanobacterial populations in shallow lakes: implications of burst size. J. Mar. Biol. Assoc. UK. 2006; 86:537–542.

Graham AL. Ecological rules governing helminth-microparasite coinfection. Proc. Nat. Acad. Sci. USA. 2008; 105:566–570. [PubMed: 18182496]

Grover, JP. Resource Competition. Chapman & Hall; London: 1997.

Gsell AS, De Senerpont Domis LH, Naus-Wiezer SMH, Helmsing NR, van Donk E, Ibelings BW. Spatiotemporal variation in the distribution of chytrid parasites in diatom host populations. Freshw. Biol. 2013; 58:523–537.

Hall SR, Knight CJ, Becker CR, Duffy MA, Tessier AJ, Caceres CE. Quality matters: resource quality for hosts and the timing of epidemics. Ecol. Lett. 2009; 12:118–128. [PubMed: 19049510]

Hoffland E, Jeger MJ, van Beusichem ML. Effect of nitrogen supply rate on disease resistance in tomato depends on the pathogen. Plant Soil. 2000; 218:239–247.

Holm NP, Armstrong DE. Role of nutrient limitation and competition in controlling the populations of *Asterionella formosa* and *Microcystis aeruginosa* in semicontinuous culture. Limnol. Oceanogr. 1981; 26:622–634.

Holt, RD. The community context of disease emergence: could changes in predation be a key driver?. In: Ostfeld, RS.; Keesing, F.; Eviner, VT., editors. Infectious Disease Ecology: Effects of Ecosystems on Disease and of Disease on Ecosystems. Princeton University Press; Princeton (NJ): 2008. p. 324-346.

Holt RD, Barfield M. Feng Z, Dieckmann U, Levin S. Within-host pathogen dynamics: Some ecological and evolutionary consequences of transients, dispersal mode, and within-host spatial heterogeneity. Disease Evolution: Models, Concepts, and Data Analyses. Providence (RI): American Mathematical Society. 2006:45–66.

Holt RD, Barfield M. Direct plant-predator interactions as determinants of food chain dynamics. J. Theor. Biol. 2013; 339:47–57. [PubMed: 23648188]

Holt RD, Roy M. Predation can increase the prevalence of infectious disease. Am. Nat. 2007; 169:690–699. [PubMed: 17427139]

Hurtado PJ, Hall SR, Ellner SP. Infectious disease in consumer populations: dynamic consequences of resource-mediated transmission and infectiousness. Theor. Ecol. 2014; 7:163–179.

Inchausti P, Ginzburg LR. Maternal effects mechanism of population cycling: a formidable competitor to the traditional predator-prey view. Philos. Trans. R. Soc. Lond., B, Biol. Sci. 2008; 364:1117–1124. [PubMed: 19324616]

Johnson PTJ, Rohr JR, Hoverman JT, Kellermanns E, Bowerman J, Lunde KB. Living fast and dying of infection: host life history drives interspecific variation in infection and disease risk. Ecol. Lett. 2012; 15:235–242. [PubMed: 22221837]

Johnson PTJ, Townsend AR, Cleveland CC, Glibert PM, Howarth RW, McKenzie VJ, Rejmankova E, Ward MH. Linking environmental nutrient enrichment and disease emergence in humans and wildlife. Ecol. Appl. 2010; 20:16–29. [PubMed: 20349828]

Kooijman, SALM. Dynamic energy budget theory for metabolic organization. Cambridge University Press; Cambridge (UK): 2010.

Lacroix C, Seabloom EW, Borer ET. Environmental nutrient supply alters prevalence and weakens competitive interactions among coinfecting viruses. New Phytol. 2014; 204:424–433. [PubMed: 24975238]

Levi T, Kilpatrick AM, Mangel M, Wilmers CC. Deer, predators, and the emergence of Lyme disease. Proc. Natl. Acad. Sci. USA. 2012; 19:10942–10947. [PubMed: 22711825]

Lloyd AL. The dependence of viral parameter estimates on the assumed viral life cycle: limitations of studies of viral load data. Proc. R. Soc. Lond. B. 2001; 268:847–854.

Mackay GA, Niu Y, Liu ZQ, Mukherjee S, Li Z, Adany I, Buch S, Zhuge W, McClure HM, Narayan O, Smith MS. Presence of intact vpu and ef genes in non-pathogenic SHIV is essential for acquisition of pathogenicity of this virus by serial passage in macaques. Virology. 2002; 295:133–146. [PubMed: 12033772]

Middelboe M. Bacterial growth rate and marine virus-host dynamics. Microb. Ecol. 2000; 40:114–124. [PubMed: 11029080]

Monier A, Welsh RM, Gentemann C, Weinstock G, Sodergren E, Armbrust EV, Eisen JA, Worden AZ. Phosphate transporters in marine phytoplankton and their viruses: cross-domain commonalities in viral-host gene exchanges. Environ. Microbiol. 2012; 14:162–176. [PubMed: 21914098]

Neumann AU, Lam NP, Dahari H, Gretch DR, Wiley TE, Layden TJ, Perelson AS. Hepatitis C viral dynamics in vivo and the antiviral efficacy of interferon-α therapy. Science. 1998; 282:103–107. [PubMed: 9756471]

Nowak, M.; May, RM. Virus dynamics: mathematical principles of immunology and virology. Oxford University Press; Oxford: 2000.

Ogura H, Sato H, Hatano M. Relation of HVJ (Sendai Virus) production to cell growth phase in persistently infected mouse 3T3 cells. Arch. Virol. 1984; 80:47–57. [PubMed: 6200094]

Packer C, Holt RD, Dobson A, Hudson P. Keeping the herds healthy and alert: impacts of predation upon prey with specialist pathogens. Ecol. Lett. 2003; 6:797–802.

Perelson AS, Nelson PW. Mathematical analysis of HIV-1: Dynamics in vivo. SIAM Review. 1999; 41:3–44.

Perelson AS, Neumann AU, Markowitz M, Leonard JM, Ho DD. HIV-1 dynamics in vivo: Virion clearance rate, infected cell life-span, and viral generation time. Science. 1996; 271:1582–1586. [PubMed: 8599114]

Pietschmann T, Lohmann V, Rutter G, Kurpanek K, Bartenschlager R. Characterization of cell lines carrying self-replicating hepatitis C virus RNAs. J. Virol. 2001; 75:1252–1264. [PubMed: 11152498]

Radford KM, Reid S, Greenfield PF. Substrate limitation in the baculovirus expression vector system. Biotechnol. Bioeng. 1997; 56:32–44. [PubMed: 18636607]

Smith MS, Niu Y, Li Z, Adany I, Pinson DM, Liu ZQ, Berry T, Sheffer D, Jia F, Narayan O. Systemic infection and limited replication of SHIV vaccine virus in brains of macaques inoculated intracerebrally with infectious viral DNA. Virology. 2002; 301:130–135. [PubMed: 12359453]

Smith VH. Resource competition between host and pathogen. BioScience. 1993a; 43:21–31.

Smith, VH. Implications of resource-ratio theory for microbial ecology.. In: Jones, JG., editor. Advances in Microbial Ecology. Vol. 13. Plenum; New York (NY): 1993b. p. 1-37.

Smith VH. Host resource supplies influence the dynamics and outcome of infectious disease. Integr. Comp. Bio. 2007; 47:310–316. [PubMed: 21672840]

Smith VH, Jones TP II, Smith MS. Host nutrition and infectious disease: An ecological view. Front. Ecol. Environ. 2005; 3:268–274.

Solomon PS, Tan K-C, Oliver RP. The nutrient supply of pathogenic fungi; a fertile field for study. Mol. Plant Pathol. 2003; 4:203–210. [PubMed: 20569380]

Tilman, D. Resource competition and community structure. Princeton Univ. Press; Princeton (NJ): 1982.

Våge S, Storesund JE, Thingstad TF. Adding a cost of resistance description extends the ability of virus–host model to explain observed patterns in structure and function of pelagic microbial communities. Environ. Microbiol. 2013; 15:1842–1852. [PubMed: 23331773]

van Donk, E.; Bruning, K. Effects of fungal parasites on planktonic algae and the role of environmental factors in the fungus-alga relationship.. In: Wiessner, W.; Schnepf, E.; Starr, RC., editors. Algae, environment and human affairs. Biopress Ltd; Bristol: 1995. p. 223-234.

van Donk E, Ringelberg J. The effect of fungal parasitism on the succession of diatoms in Lake Maarsseveen I (The Netherlands). Freshw. Biol. 1983; 13:241–251.

Wilson WH, Carr NG, Mann NH. The effect of phosphate status on the kinetics of cyanophage infection in the oceanic cyanobacterium *Synechococcus* sp. WH7803. J. Phycol. 1996; 32:506–516.

Wodarz D. Ecological and evolutionary principles in immunology. Ecol. Lett. 2006; 9:694–705. [PubMed: 16706914]

Wu JT, Byrne HM, Kirn DH, Wein LM. Modeling and analysis of a virus that replicates selectively in tumor cells. Bull. Math. Biol. 2001; 63:731–768. [PubMed: 11497166]

You L, Suthers PF, Yin J. Effects of *Escherichia coli* physiology on growth of phage T7 in vivo and in silico. J. Bacteriol. 2002; 184:1888–1894. [PubMed: 11889095]

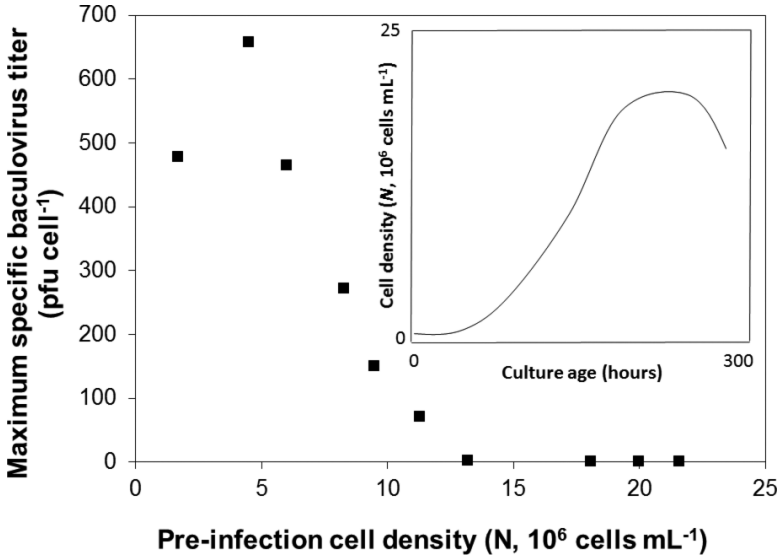

Figure 1.

Strong density dependence of maximum recombinant baculovirus production per cell in Sf9 *Spodoptera frugiperda* insect cells cultivated in laboratory batch cultures. The cell population densities depicted on the abscissa represent the initial pre-infection cell densities. Growth medium was not replaced prior to baculovirus infection of samples collected at each time point, and thus host cells in each infection experiment exhibited the resource state corresponding to 10 different sampling times along the cell population's growth curve (see inset). Data obtained and reanalyzed from Table I in Radford et al. (1997).

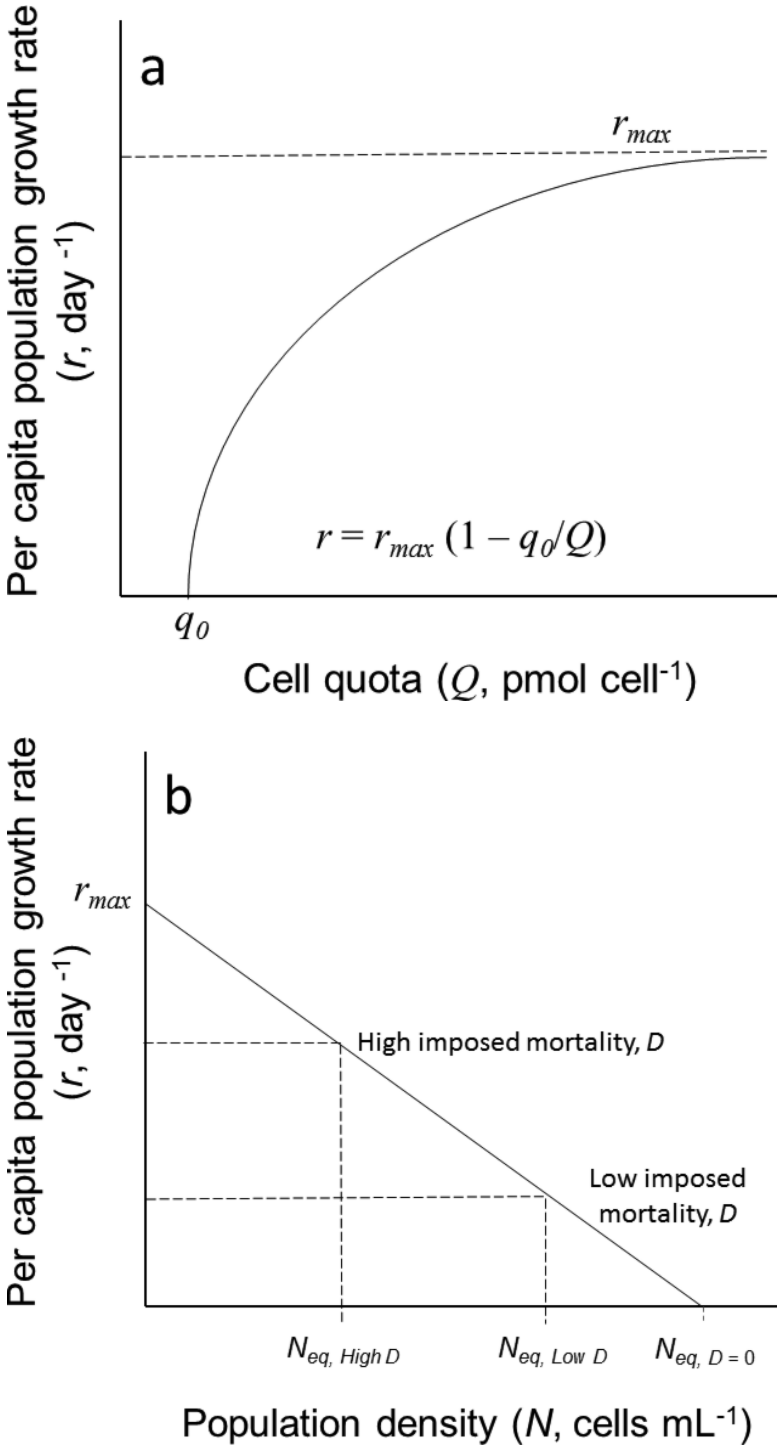

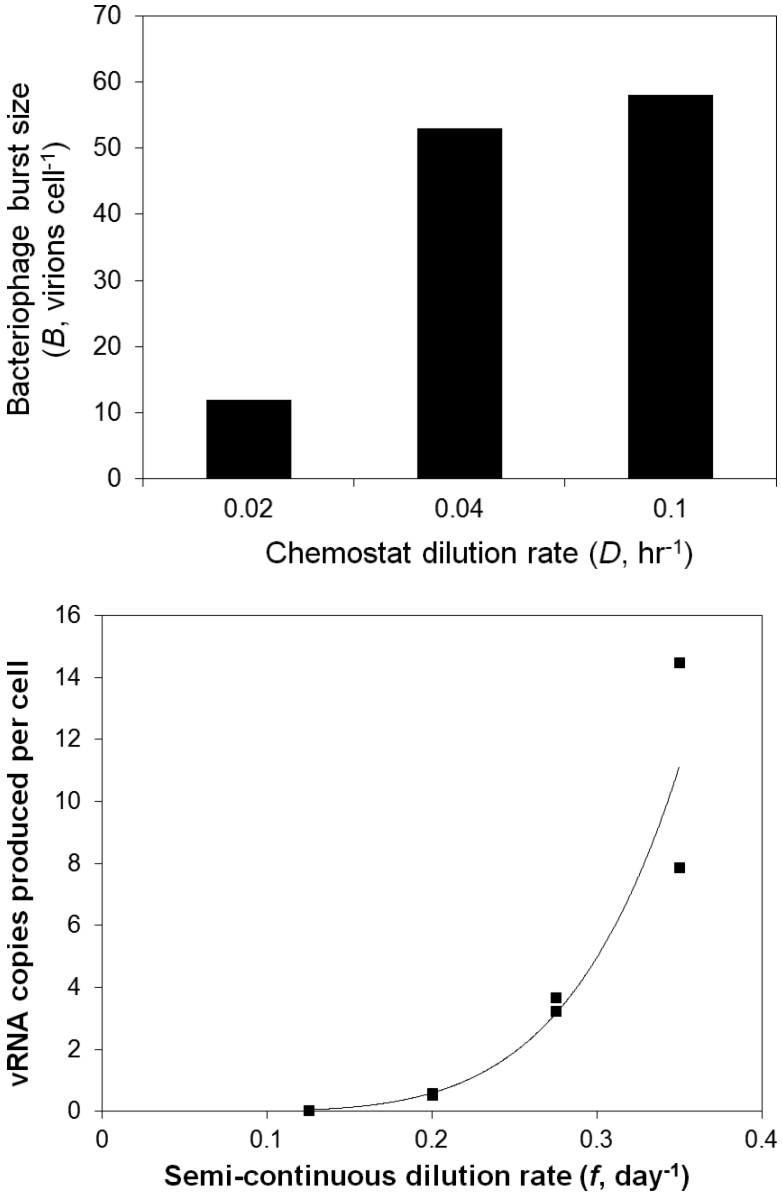

Figure 2.

(a) Hyperbolic relationship between per capita growth rates of a cell population (r, day^{-1}) and the intracellular concentration or cell quota (Q, pmol cell^{-1}) of the growth-limiting nutrient (Droop 1974). The term q_0 is the subsistence cell quota at which the birth rate of the cell population just offsets mortality losses and thus $r = 0$. (b) Inverse relationship between per capita growth rates of a cell population (r, day^{-1}) and cell population size (N, cells mL^{-1}) for logistic growth. (c) Relationship between the burst size (B, virions released per infected cell) of bacteriophage viruses and the pre-infection per capita growth rate of *Pseudoalteromonas sp.* bacterial populations cultivated in chemostat cultures at three different dilution rates. Data from Table 3 in Middelboe (2000). (d) The post-infection production of SHIV, as measured by the number of viral RNA (vRNA) copies in the supernatant that were produced per CEM cell, was a strongly positive power function of the

semi-continuous dilution rate f, which was experimentally varied from 0.125 to 0.350 day^{-1}. The non-linear least-squares regression equation for this relationship is: vRNA = 2687 $D^{5.23}$, r^2 = 0.99.

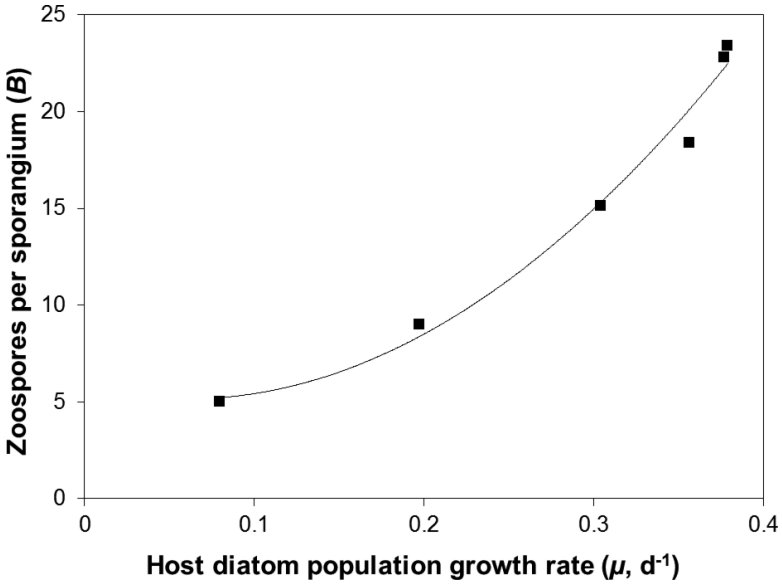

Figure 3.

Relationship between zoospore production by the chytrid fungus pathogen *Rhizophydium planktonicum* and the light-dependent per capita population growth rate of its freshwater diatom host, *Asterionella formosa*. The non-linear regression equation for this relationship is: $B = 169.5\ \mu^2 - 20.0\ \mu + 5.7$, $r^2 = 0.98$. Original data digitized and statistically reanalyzed from Bruning (1991a).

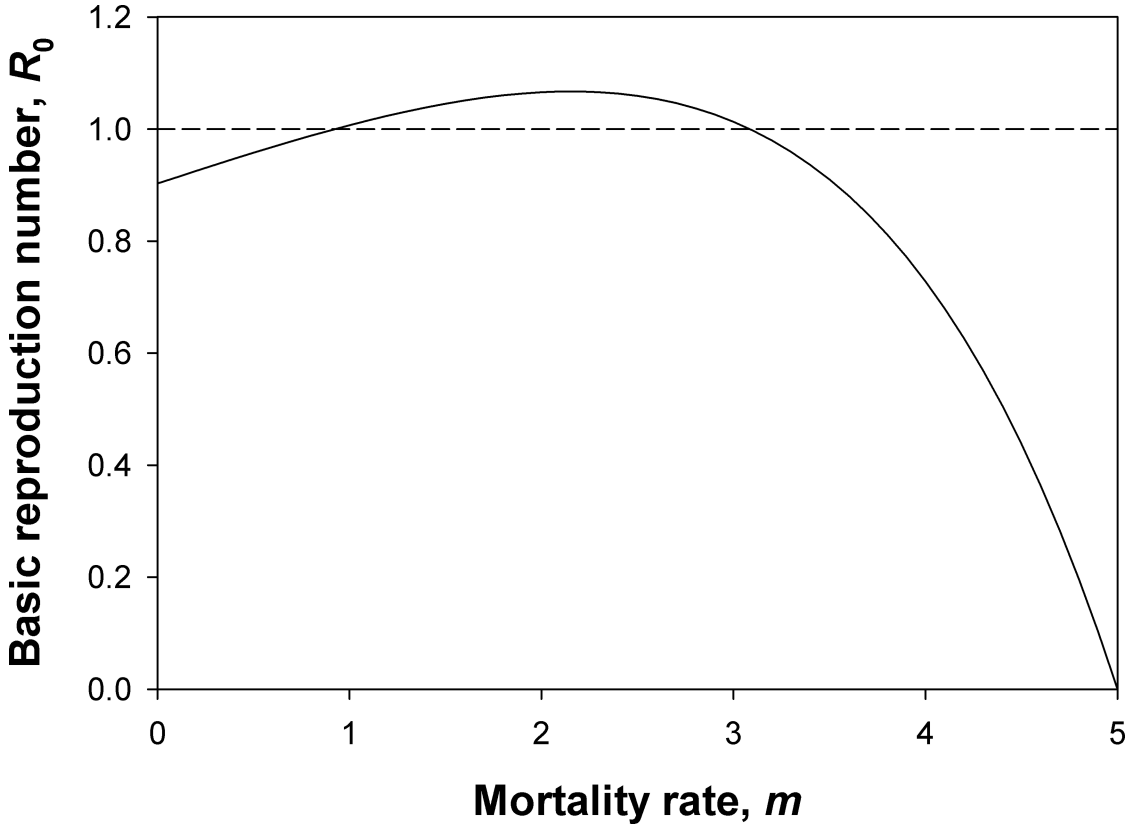

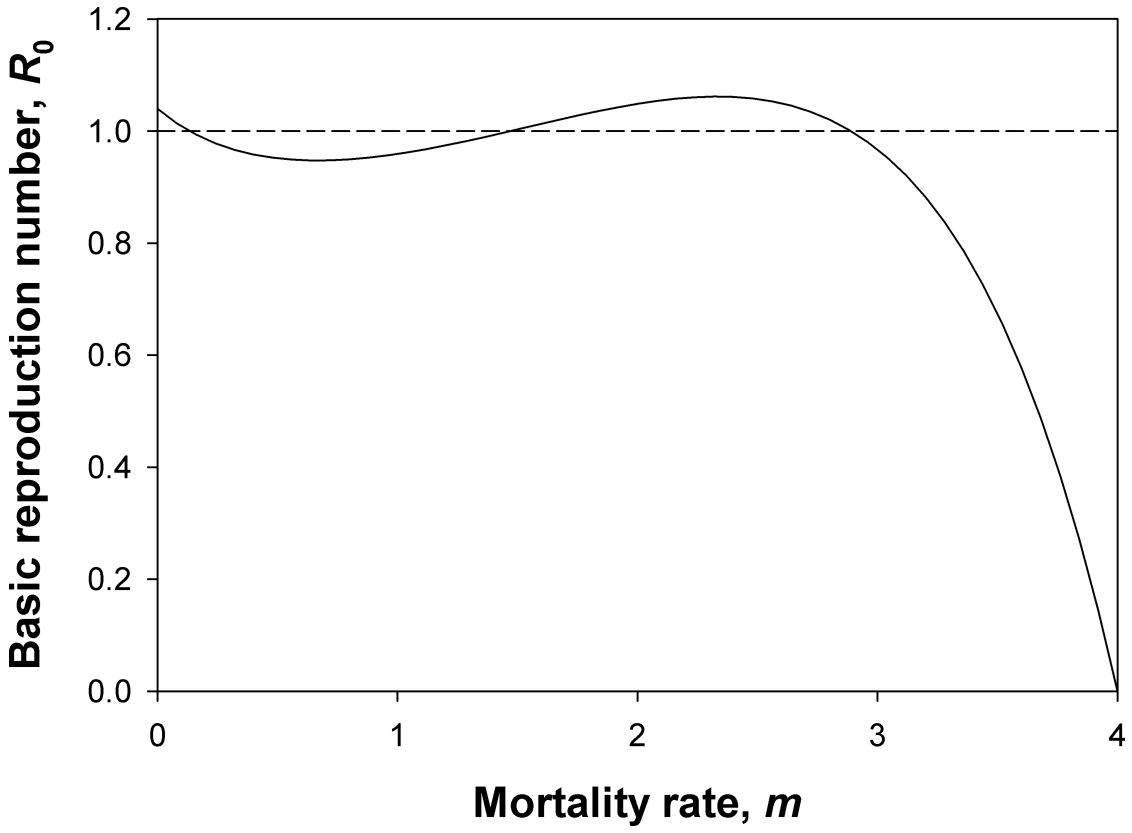

Figure 4.

Basic reproduction number as a function of mortality rate for system of Equations (4) and (5) with $\beta'(m) = \beta_0' exp\{km\}$ and parameters (a) $b = 5$, $a = 8$, $c = 0.09$, $\beta_0' = 0.13$, $k = 0.45$, or (b) $b = 4$, $a = 1$, $c = 0.1$, $\beta_0' = 0.026$, $k = 0.9$.

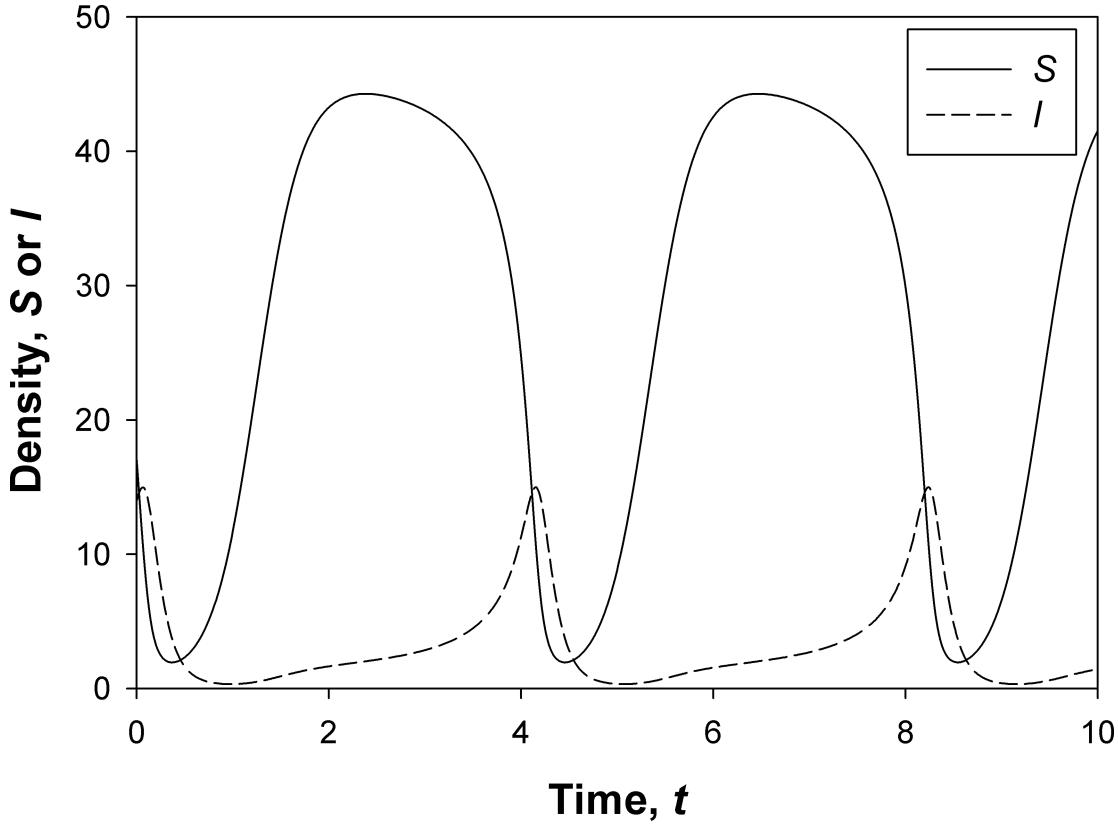

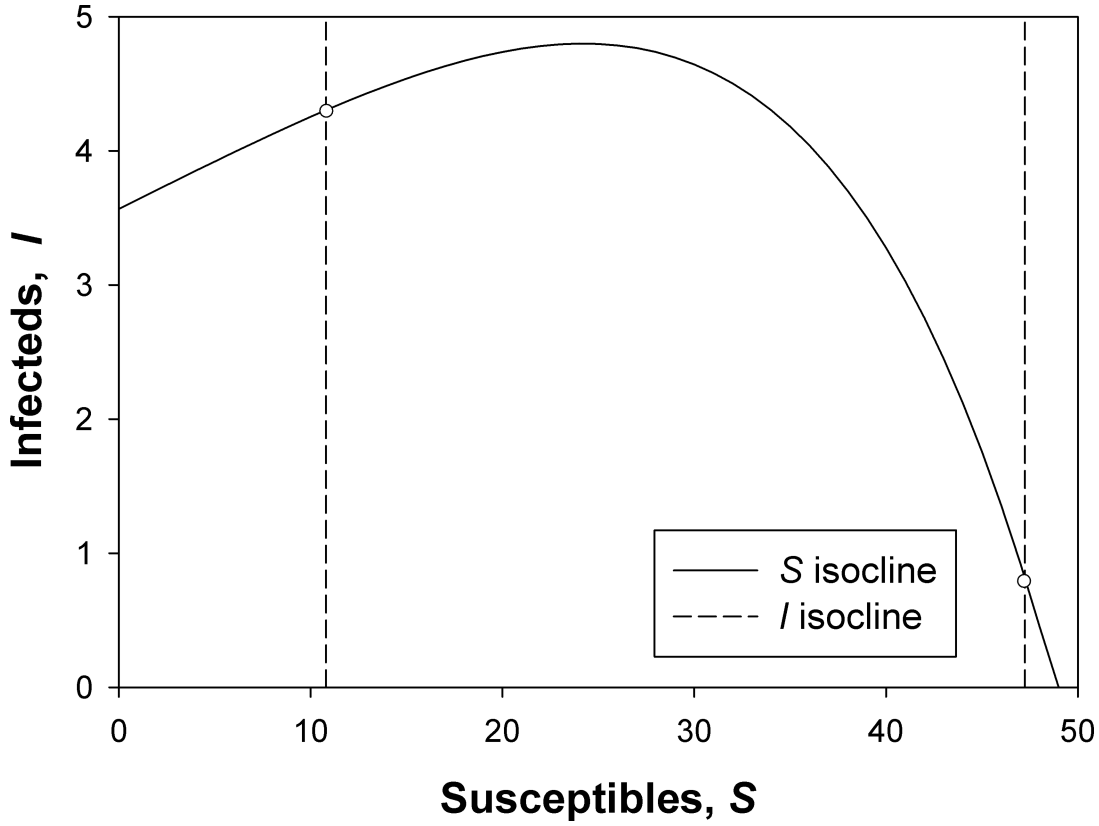

Figure 5.

(a) Cycles for system of Equations (4) and (5) with $m = 0.6$; other parameters as in Figure 4(a). (b) Isoclines for this system of equations. Both equilibria (open circles) are unstable. If the system is started near the right equilibrium, the result can be pathogen extinction or cycles around the left equilibrium (such as those shown in panel a).

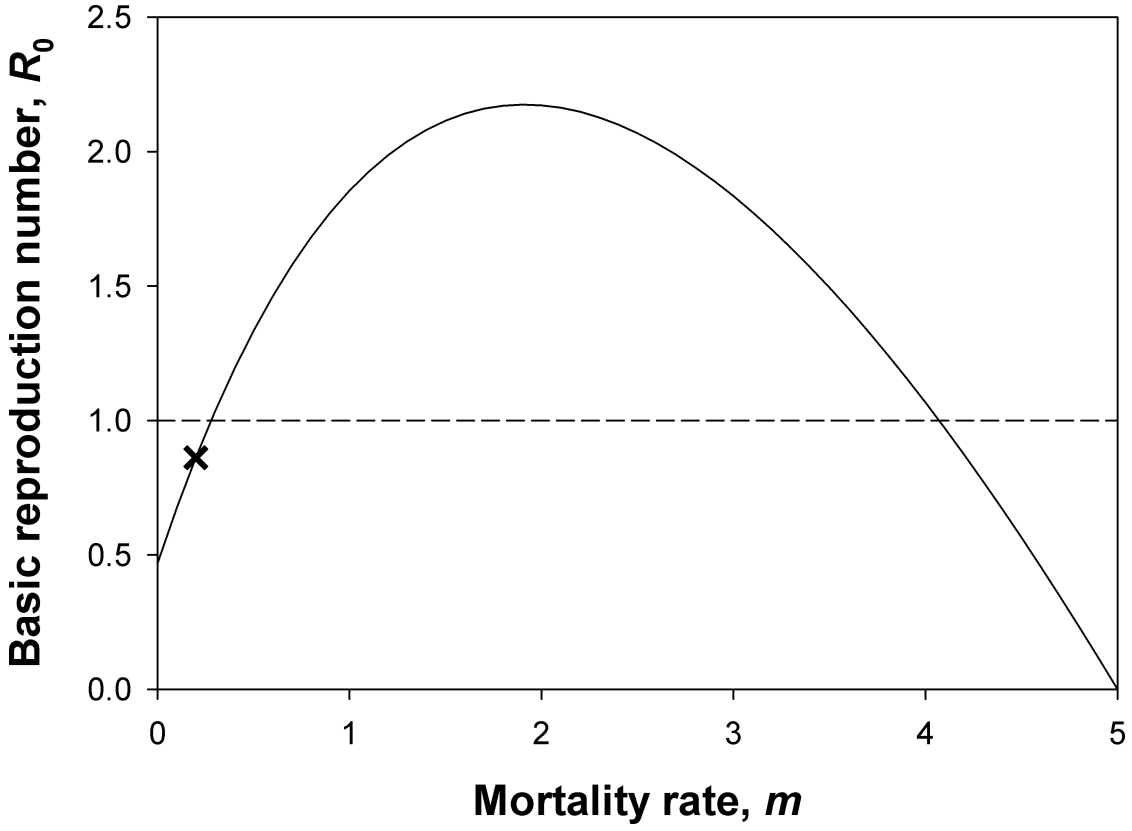

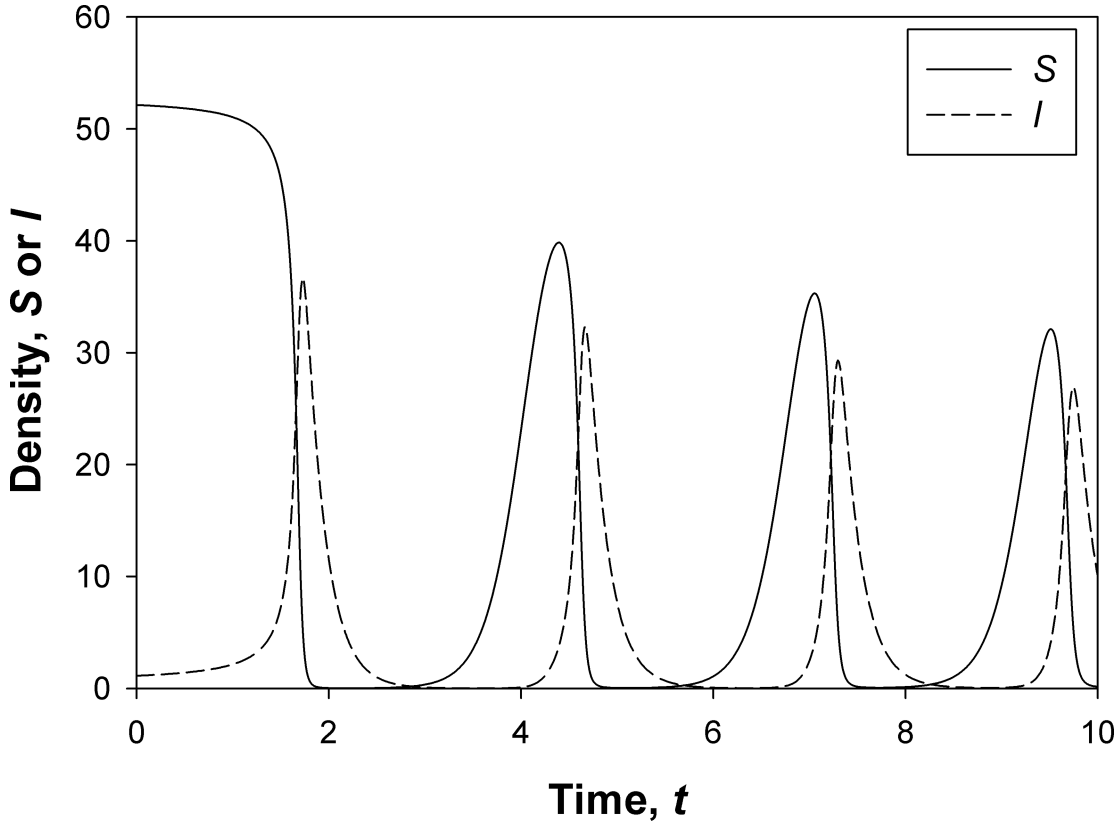

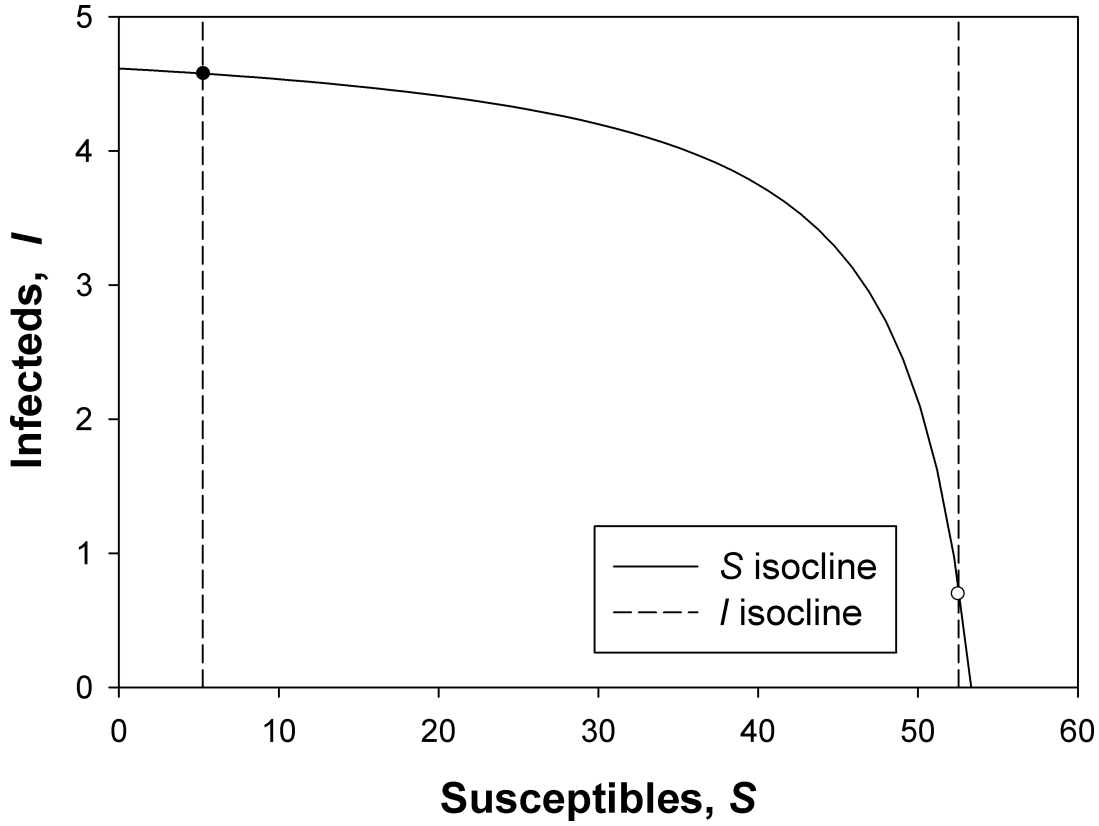

Figure 6.

(a) Basic reproduction number as a function of mortality rate for system of Equations (4) and (5) with $\beta'(g) = \beta_0' + kg$. Parameters are $b = 5$, $a = 4.75$, $c = 0.09$, $\beta_0' = 0.04$, $k = 0.2$. (b) Trajectories of S and I for this system started near the equilibrium with higher S^*. The system eventually settles at the stable equilibrium at $S^* = 5.234$ and $I^* = 4.577$. For other initial values near the higher S^* equilibrium, the pathogen is lost. The mortality rate is $m = 0.2$, indicated by the × in panel (a); other parameters as in panel (a). (c) Isoclines for this system with parameters of panel (b). The right equilibrium is unstable (open circle) and the left one is stable (filled circle).

Table 1

Examples of virus-host systems in which host population growth rate or growth stage has been observed to have strong effects upon viral replication rate.

Virus	**Host**	**Virus group**	**Reference**
Sendai virus (SeV, HVJ)	mouse fibroblasts	(−)ssRNA	Ogura et al. (1984)
hepatitis C virus (HCV)	human hepatoma cells	(+)ssRNA	Pietschmann et al. (2001)
Phaeocystis pouchetii virus (PpV01)	*Phaeocystis pouchetii* (marine alga)	dsDNA	Bratbak et al. (1998)
vaccinia virus (VACV)	HeLa cells	dsDNA	Chillakuru et al. (1991)
bacteriophage T7	*E. coli* BL21 (Gal^{-} λ^{S} *hsdS*) cells	dsDNA	You et al. (2002)